Pd nanoparticles prepared by "controlled colloidal synthesis" in solid/liquid interfacial layer on silica. I. Particle size regulation by reduction time

A. Beck [a], A. Horváth [a], A. Szűcs [b], Z. Schay [a], Z.E. Horváth [c], Z. Zsoldos [a], I. Dékány [b] and L. Guczi [a]

[a] *Department of Surface Chemistry and Catalysis, Institute of Isotope and Surface Chemistry, Chemical Research Center, Hungarian Academy of Sciences, PO Box 77, H-1525 Budapest, Hungary*
[b] *Department of Colloid Chemistry, Attila József University, Aradi Vértanuk tér. 1, H-6720 Szeged, Hungary*
[c] *Institute of Technical Physics and Materials Science, PO Box 49, H-1525 Budapest, Hungary*

Received 1 April 1999; accepted 10 January 2000

Controlled colloidal synthesis (CCS) was developed to prepare monodisperse palladium particles in the nano-scale range on suspended SiO_2 particles in an ethanol–toluene mixture. On colloidal SiO_2 an about 1 nm thick ethanol-rich adsorption layer was produced in adsorption equilibrium with the liquid mixture. Ethanol served as a reducing agent for the Pd(II) ions diffusing from a toluene-rich liquid solution into the interfacial layer. The low reduction rate ensures the dominancy of particle growth over the nucleation of palladium during the reduction process after the initial nucleation. The relation between the reduction time and the particle size produced was studied. XRF, XPS, TEM, CO chemisorption, and benzene hydrogenation as catalytic test were employed to characterize the samples prepared using different reduction time.

Keywords: controlled colloidal synthesis (CCS), preparation of Pd nanoparticles, structure and activity of Pd particles

1. Introduction

General ambition in catalyst preparation is to design and produce tailor made catalysts with well defined structure. The structure involves a great deal of different characteristics, but for supported catalysts the particle size and the particle size distribution are the two most important parameters. Particle size effect on catalytic performance of heterogeneous metal catalysts has been widely and systematically studied for more than twenty years, but it is still an intriguing problem and several new findings can be highlighted [1]. By the development of the experimental techniques, the different parameters can be determined and controlled more precisely and more genuine correlations can be revealed. Metal particles smaller than 1–3 nm in diameter, have special interest for the borderline between metallic and molecular state and they have a unique electronic structure which also affects catalytic properties [2]. Once we are possessing monodisperse metal particles on a support, the specificity of the different sizes can be studied and the effects on catalysis can be elucidated more precisely.

Different preparation techniques provide several chances to control the particle size and to form size distribution in a narrow size region. Precursors containing preformed, well defined metal clusters, e.g., transition metal carbonyl clusters, after deposition and decomposition on the support can be applied to produce well defined dispersed metal particles provided that they retain the intact, ligand-free metal framework. A large number of works done in this field, showed a complex character of these systems, because in most cases the original metal framework undergoes decomposition interacting with the support [3].

The same concept applies to monodisperse metal-sol as precursor [4]. In this case metal particles are larger than those in metal clusters, however, after removing the stabilizing agents it is still doubtful whether or not the original metal distribution is retained.

Spatial restriction of the particle growth can also govern generation of a monodisperse metal system. During reduction of the metal ions in a well defined pore structure of zeolites, the particle growth could be controlled, but sometimes it is a problem to prevent particle migration to and growth at the external surface of the zeolite. Growth of the particles into the neighbouring channels and pores producing "grape-shaped" metal arrays, is also a well known phenomenon [5].

In microemulsions the metal ions are separated in micelles and this controls the particle growth and prevents aggregation of the particles [6]. Highly dispersed metal particles can be deposited on a support, but the generation of metal and support particles in the same micelles is also possible. Problems arise again how the removal of the solvents and surfactants which stabilize the monodispersed particles, affects the stability of the system.

Controlling the particle growth itself on the support surface results in the formation of monodispersed metal particles. There are sophisticated and technically complicated methods, such as metal vapor deposition, laser pulse deposition, photo- and electron-lithography which provide tailored metal particles and in the case of the lithography the array

of the particles can also be designed [7]. These methods are suitable for preparation of model systems.

The *in situ* generation of metal particles at the solid/liquid interfacial layer on a support, where concentration of the reducing agent and the metal salts can be regulated, could give a chance for controlling the average particle size of the metal phase. A synthetic route has been developed for *in situ* generation of palladium particles in the adsorption layer of hexadecylammonium montmorillonite [8] and CdS and ZnS semiconductor nanoparticles in the adsorption layer of hexadecylpyridinium montmorillonite [9] and colloidal silica particles [10] suspended in a binary solvent system.

Principle of the preparation method

The controlled colloidal synthesis (CCS) is postulated by the procedure of reduction of a precursor localized in a well designed solid/liquid interfacial layer on the support. Using a proper binary liquid system for the suspension of the support good separation can be achieved between the adsorption layer and the liquid phase for one of the two components, so the liquid phase contains it in negligible concentration. If one of the reaction partners is soluble only in this component, or this component itself is the reducing agent, the reduction is localized.

When the reduction rate is small enough, the nucleus growth can dominate over negligible nucleus formation and so the growth of the nuclei formed in the initial nucleation can be performed. The nuclei probably are growing with similar rate, provided that the reduction rate is uniform overall the surface namely the temperature is uniform and reducing agent and precursor ions are uniformly distributed along the surface.

Use of different reduction times seems to be a possible way of particle size control. Another possibility for particle size control is the regulation of the initial nucleation producing different number of nuclei.

In the present work we aim to adopt the method postulated to prepare monodisperse Pd nanoparticles on silica support and to study the possibility to regulate the particle size and its distribution by the reduction time.

2. Experimental

2.1. Materials

Hydrophilic colloidal silica (SiO_2) A-200 (average particle diameter is 12 nm) was obtained from Degussa (Germany). Pd(II) acetate, $Pd(OAc)_2$ and Pd(II) chloride, $PdCl_2$ were purchased from Merck and used as received. Ethanol and toluene (Reanal, Hungary) were distilled and stored over a 0.4 nm molecular sieve (Merck AG, Germany). For catalytic test benzene destilled and hydrogen purified on Pd/Al_2O_3 and on zeolit 5A were used.

2.2. Sample preparation

In the preparation procedure of samples CCS 1–5 1 g of SiO_2 previously kept in a vacuum desiccator at 333 K for 3 h, was suspended in 100 cm^3 ethanol : toluene = 6 : 94 mixture. After the adsorption equilibration had been attained (ca. 10 h), 30 cm^3 of 1 m/m% of Pd acetate toluene solution was added to the system. The suspension was stirred with magnetic device and the reaction was allowed to proceed at room temperature. After different time the reduction process was stopped, the Pd/SiO_2 was purified in toluene by several centrifugation–redispersion cycles and thus the Pd(II) acetate not reduced, was removed. The samples were dried at room temperature. For reference sample IMP A SiO_2 was impregnated with aqueous solution of $PdCl_2$, dried at 353 K, calcined at 773 K in O_2 then reduced at 773 K in H_2 stream for 3 h, for IMP B SiO_2 was impregnated with toluene solution of $Pd(OAc)_2$, dried at room temperature and reduced at 423 K in H_2 stream for 90 min. The Pd content of the samples was determined by X-ray fluorescence technique.

2.3. Determination of the adsorption isotherms of the ethanol–toluene–A200 system

Silica particles were allowed to equilibrate with a given liquid mixture (298 K, 48 h) and the composition of supernatant liquid was determined by a Zeiss liquid interferometer. The excess isotherms were calculated by the equation

$$\begin{aligned} n_1^{\sigma(n)} &= n^0\big(x_1^0 - x_1\big)/m = n_1^{\mathrm{s}} - \big(n_1^{\mathrm{s}} + n_2^{\mathrm{s}}\big)x_1 \\ &= n_1^{\mathrm{s}}x_2 - n_1^{\mathrm{s}}x_1 = n^{\mathrm{s}}\big(x_1^{\mathrm{s}} - x_1\big), \end{aligned} \tag{1}$$

where $n_1^{\sigma(n)}$ is the adsorption excess amount per gram of adsorbent, x_1^0 is the initial, x_1 is the equilibrium composition of the liquid phase, n^0 is the number of moles in the liquid mixture in the dispersed system, $n_1^{\mathrm{s}} + n_2^{\mathrm{s}} = n^{\mathrm{s}}$ is the material content of the adsorption layer and $x_1^{\mathrm{s}} = n_1^{\mathrm{s}}/n^{\mathrm{s}}$ is the mole fraction of the adsorption layer.

The volume of the adsorption layer was calculated using the Williams equation

$$V^{\mathrm{s}} = n_1^{\mathrm{s}}V_{\mathrm{m},1} + n_2^{\mathrm{s}}V_{\mathrm{m},2}, \tag{2}$$

where V^{s} is the volume of the adsorption layer, $V_{\mathrm{m},1}$, $V_{\mathrm{m},2}$ are the molar volumes of the adsorbed components 1 and 2. If we have preferential adsorption of component 1 ($n_1^{\mathrm{s}} \gg n_2^{\mathrm{s}}$), $V^{\mathrm{s}} = n_{1,0}^{\mathrm{s}}V_{\mathrm{m},1}$, where $n_{1,0}^{\mathrm{s}}$ can be determined by linear extrapolation from the linear section of the adsorption excess isotherm after Schay and Nagy [11].

2.4. Rheological measurements

Shear stress (τ) versus shear rate gradient (D) was monitored in the range 0–100 s^{-1} for the SiO_2 and Pd/SiO_2 suspension (2% in toluene) using a "low shear" Haake rotational viscosimeter (RV20-CV100).

2.5. Transmission electron microscopy

One drop of an ultrasono-mixed, dilute toluene suspension of the "as-prepared" (see section 2.2) samples was placed on a carbon-coated grid and after evaporation of the solvent electron micrographs of the particles retained were taken. A Philips CM20 microscope operating at 200 kV equipped by an energy dispersive spectrometer (EDS) was used.

2.6. X-ray photoelectron spectroscopy (XPS)

The oxidation state of Pd was determined by XPS performed by a KRATOS XSAM 800 XPS machine equipped with an atmospheric reaction chamber. Spectra were taken on the "as-prepared" (see section 2.2) samples and on those subsequently treated in hydrogen at 423 and 573 K for 1 h each. Mg Kα excitation was used. The binding energies were determined relative to Si 2p at 103.3 eV. For the surface composition signals of Pd 3d, O 1s, Si 2p, and C 1s were considered using the sensitivity factors given by the manufacturer.

2.7. CO chemisorption

CO chemisorption was measured in a pulse-flow system type SORBSTAR equipped with a thermal conductivity detector. CO pulses in an argon stream were used at room temperature after a treatment in hydrogen at 423 K for 1 h.

2.8. Catalytic reaction

Benzene hydrogenation was studied in a flow reactor working in differential regime. The effluent was analysed by a gas chromatograph type Chrompack 437 using a squalan/chromosorb W column. The benzene content of the 1 atm hydrogen stream was set by a saturator at 273 K, the component ratio was $H_2/C_2H_6 = 37$. Reaction rate was measured at different temperatures between 373 and 443 K after treatment in hydrogen stream at 423 K for 1 h.

3. Results

In figure 1 the adsorption isotherms of the A200–ethanol–toluene system are presented. On this basis one can determine the composition, the volume and the thickness of the adsorption layer. In the preparation procedure used, the mole fraction of ethanol in the liquid phase (x_1) and in the adsorption layer (x_1^s) was 0.09 and 0.9, respectively. Taking into account the volume of the adsorption layer $V^s = 0.17$ cm^3/g calculated by equation (2) and the specific surface area of A200 ($A_s = 197$ m^2/g), the thickness of the adsorption layer was about $t^s = V^s/A_s = 0.9$ nm.

The metal contents of the Pd/SiO_2 samples determined by XRF spectroscopy are presented in table 1. About 1–10% of the palladium acetate in the synthesis mixture was reduced in the case of CCS 1–5.

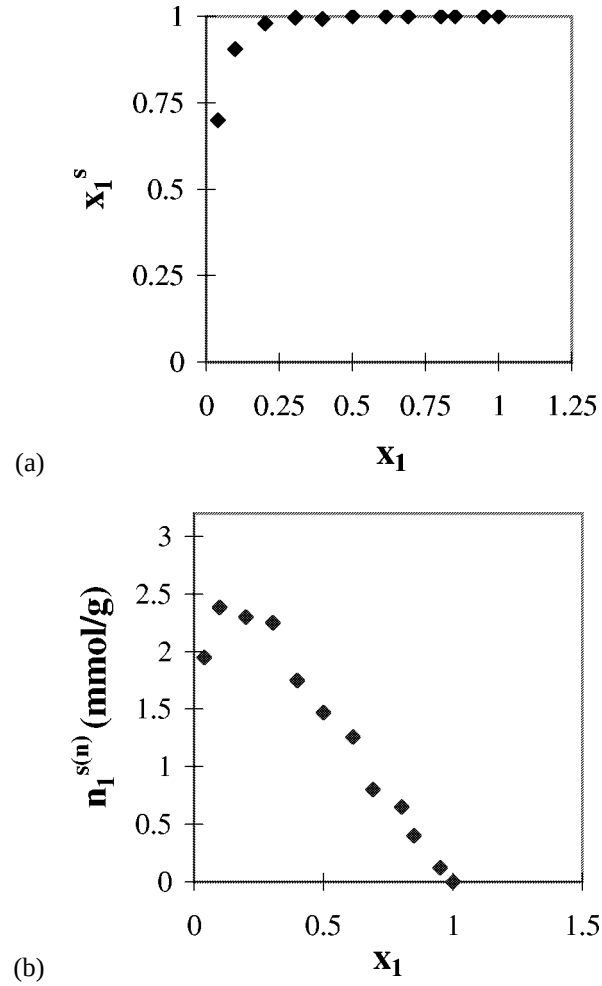

Figure 1. Adsorption isotherms of the ethanol(1)–toluene(2)–A200 system.

Formation of Pd particles on SiO_2 affected the rheological properties of the SiO_2 suspension as it is visible from the flow curves of toluene suspension of the pure SiO_2 and the Pd/SiO_2 plotted in figure 2. The Bingham yield value, τ_B, increases with the formation of Pd(0).

The Pd and SiO_2 particles in the "as-prepared" Pd/SiO_2 samples are shown by TEM. In figure 3 (a) and (b) pictures of two different systems are presented. Measuring the particle diameter of all Pd particles photographed the distribution histograms of the particle size were produced for each system (figure 4) and the average particle diameters with the standard deviations of the systems were calculated and indicated in table 1. From the average particle diameter the Pd dispersion was calculated assuming spherical polycrystalline particles where the estimated Pd surface density is 12.7 Pd/nm [12]. The particle size distribution is significantly narrower in the samples prepared by CCS than in sample IMP A.

In figure 5 the XPS spectra of the "as-prepared" and the treated Pd/SiO_2 samples prepared by CCS can be seen. Table 2 shows the binding energies of the Pd $3d_{5/2}$ peaks and the "surface concentration" of palladium and carbon calculated from the spectra. On the samples XPS did not show

Table 1
Experimental and some calculated data of Pd/SiO_2 samples.

Sample	Reduction time	Pd content		Pd dispersion[a] (%)		Pd particle diameter[b] (nm)		Catalytic activity[c] (1/s)		Activation energy
	(min)	(m/m%)	(μmol/g_{cat})	$D_{CO\,ads}$	D_{TEM}	$d_{CO\,ads}$	$d_{TEM} \pm \sigma$	$TON_{CO\,ads}$	TON_{TEM}	(kJ/mol)
CCS 1	90	0.27	25	18	19	6	6 ± 2.3	0.017	0.016	33
CCS 2	180	0.49	46	20	12	6	9 ± 3.6	0.022	0.037	43
CCS 3	180	0.52	48	8	19	13	6 ± 2.5	0.012	0.005	36
CCS 4	240	0.74	69	11	16	10	7 ± 2.4	0.022	0.016	39
CCS 5	720	1.50	141	4	14	26	8 ± 2.5	–	–	–
IMP A		1.85	174	7	9	17	13 ± 7.5	0.017	0.013	44
IMP B		0.41	39	22	16	5	7 ± 3.4	0.017	0.024	33

[a] $D_{CO\,ads}$: dispersion of palladium determined by CO chemisorption; D_{TEM}: dispersion of palladium calculated from the particle diameter measured by TEM.
[b] $d_{CO\,ads}$: particle diameter calculated from the CO chemisorption data; d_{TEM}: particle diameter determined by TEM.
[c] $TON_{CO\,ads}$: turnover number of benzene to cyclohexane (393 K, $H_2/C_2H_6 = 37$) calculated by $D_{CO\,ads}$; TON_{TEM}: turnover number of benzene to cyclohexane (393 K, $H_2/C_2H_6 = 37$) calculated by D_{TEM}.

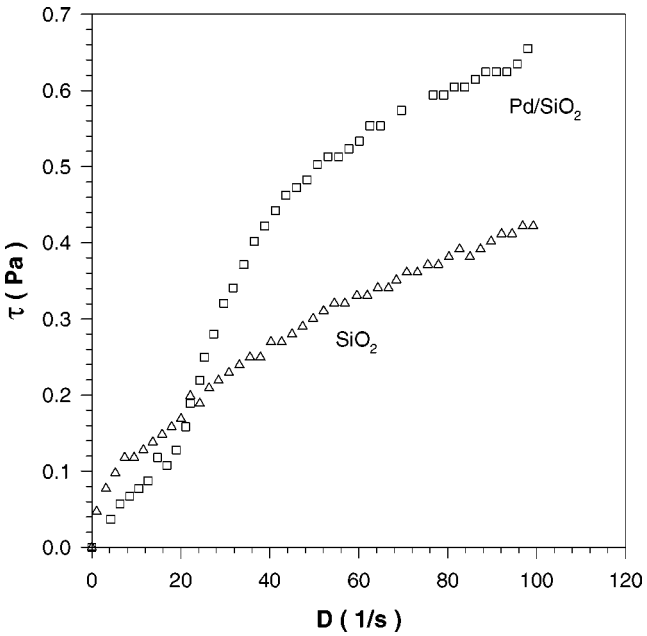

Figure 2. Flow curves of toluene suspension of SiO_2 and Pd/SiO_2 prepared by CCS.

components other than silicon, oxygen, palladium and carbon. The carbon content of the Pd/SiO_2 was not higher than that on the pure silica. The characteristic Pd 3d peaks for the "as-prepared" sample seem to be a superposition of the peaks of different Pd states, and on the effect of heat treatment in a stream of H_2 the bands shifted to lower binding energy indicating the reduction of Pd. A 0.4 eV shift had occurred at 423 K, and the subsequent heating in hydrogen at 573 K caused no significant additional shift.

CO chemisorption was used to determine the fraction of palladium exposed to the surface. The amount of CO chemisorbed on the "as-prepared" samples after treatment at 423 K in hydrogen for 60 min was measured. The dispersion of palladium presented in table 1 was estimated with the assumption that CO was chemisorbed partly in linear and partly in bridged form and the average stoichiometry of the chemisorption is $Pd:CO = 1.5$. This assumption was

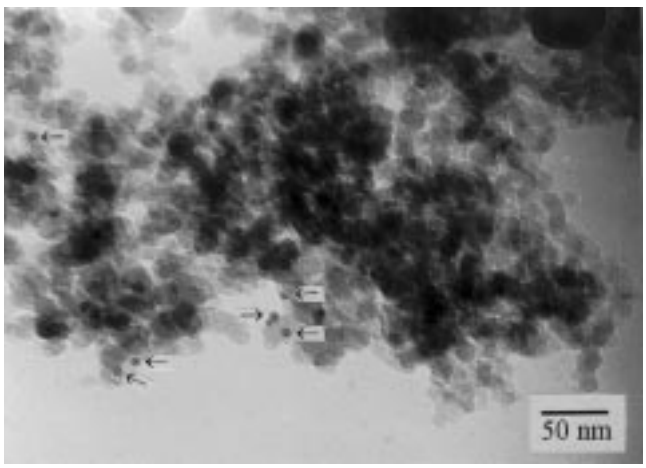

(a)

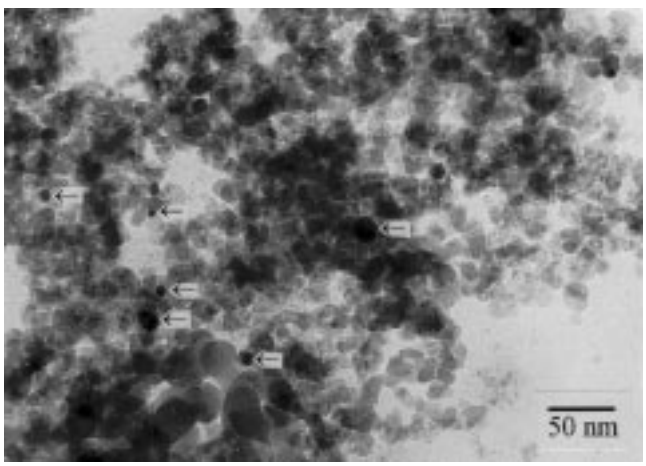

(b)

Figure 3. TEM pictures of Pd/SiO_2 samples: (a) CCS 4 and (b) IMP A (some of the Pd particles are marked with arrows).

based on the literature data measured on SiO_2-supported Pd with similar metal dispersion [13]. The average particle diameter (see table 1) was calculated from the dispersion measured by CO chemisorption assuming spherical polycrystalline particles.

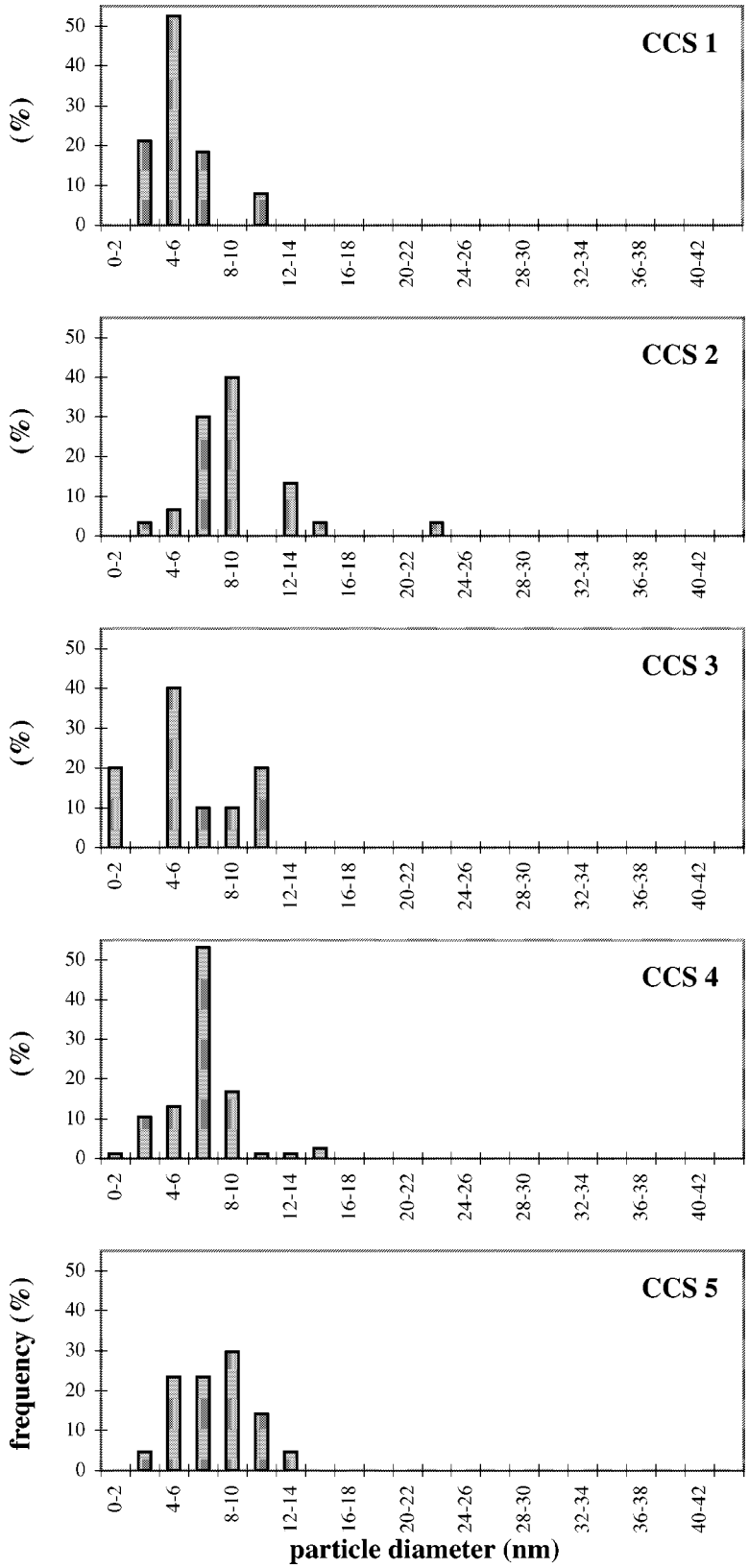

Figure 4. Palladium particle size distribution of the different Pd/SiO_2 samples.

The samples were tested in the hydrogenation of benzene. Measurements were done at about 1–5% conversion. The catalyst produced only cyclohexane and showed stable performance for at least 5–6 h, except with CCS 5, which deactivated after several minutes above about 423 K. The apparent activation energies were calculated on the basis

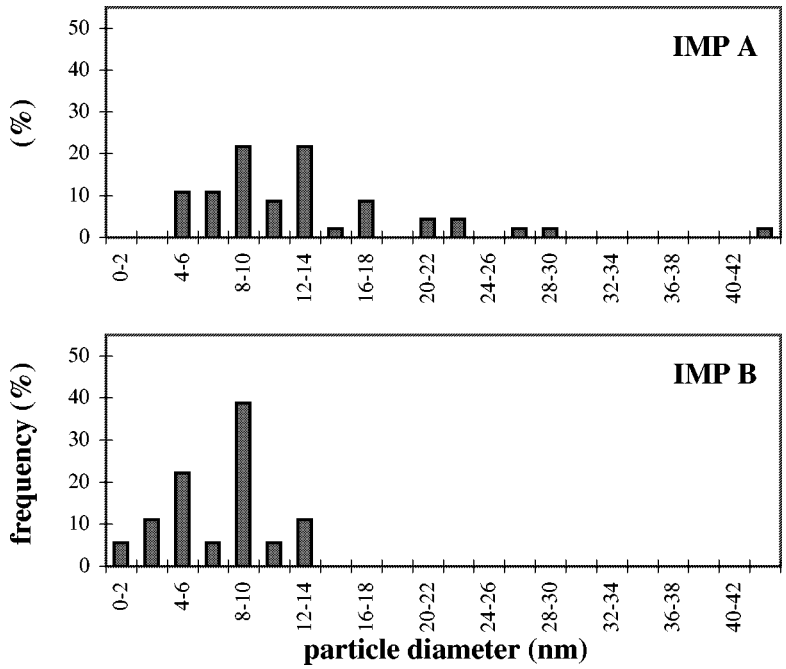

Figure 4. (Continued.)

Table 2
XPS data of Pd/SiO_2 prepared by CCS.

Treatment	Binding energy (eV)	FWHM (eV)	Surface concentration (m/m%)	
			Palladium	Carbon
"As-prepared" state	335.4	2.703	0.08	0.73
150 °C/H_2/1 h	335.1	2.082	0.07	1.76
300 °C/H_2/1 h	335.0	2.167	0.07	1.60
A200			0	2.94

of the reaction rate measured at different temperatures and collected in table 1. The turnover numbers presented also in table 1 were calculated from the reaction rates measured at 393 K using the dispersion data determined either from CO chemisorption ($TON_{CO\,ads}$), or the average particle size measured by TEM (TON_{TEM}). The activation energy varies between 33 and 44 kJ/mol including the impregnated samples, as well. There is no significant trend in the calculated $TON_{CO\,ads}$ data, which is expected since benzene hydrogenation is a structure insensitive reaction [1]. However, TON_{TEM} data show anomaly.

4. Discussion

In the controlled colloidal synthesis (CCS) performed in this work the Pd-acetate precursor was reduced by ethanol. Formation and growth of Pd particles took place predominantly in an about 1 nm thick ethanol-rich ($x_1^s = 0.9$) adsorption layer on silica particles regarding that ethanol was present in a low concentration ($x_1 = 0.09$) in the toluene/ethanol liquid phase, where the reduction of Pd(II) ions occurred to a likely negligible extent. The Pd acetate located overwhelmingly in the toluene/ethanol liquid phase, migrated through the interface onto the equilibrated adsorption layer on the silica surface and it was reduced by ethanol as it is presented in scheme 1.

The reduction process likely proceeds in the following way. The starting complex is attacked by ethoxide ions generating thereby Pd^+–OCH_2CH_3 species followed by hydrogen transfer to the metal ions with concomitant liberation of CH_3CHO species. The Pd^+–H species lose a proton which results in formation of zero-valent palladium [14]. The Pd^0 nuclei formed are deposited on the support and they provide a nucleation center for the growth of the palladium particles.

The metallic Pd particle formation generated stronger interparticle interactions which was indicated by the change of the flow curves (figure 2). Pd bridging to the neighbouring SiO_2 aggregates formed a cohesive three-dimensional network. Scheme 2 gives a schematic illustration of the proposed arrangement of the Pd and SiO_2 particles in the Pd/SiO_2 systems. TEM pictures (figure 3) show similar arrangement of the metal and support particles (having similar particle size) as it is suggested on the basis of rheological behaviour of the systems.

The Pd content detected by XPS was about one quarter of the bulk concentration. This can be explained by the proposed arrangement of the Pd and SiO_2 particles as the inelastic mean free path for Pd 3d and Si 2p photoelectrons is about the same and the diameter of the Pd and SiO_2 particles is about the same, too.

XPS measurements indicated that the Pd(II) ions were not fully reduced in the samples prepared by CCS, but they could be reduced at about 423 K. The samples must have always been reduced in the freshly prepared form, thus it

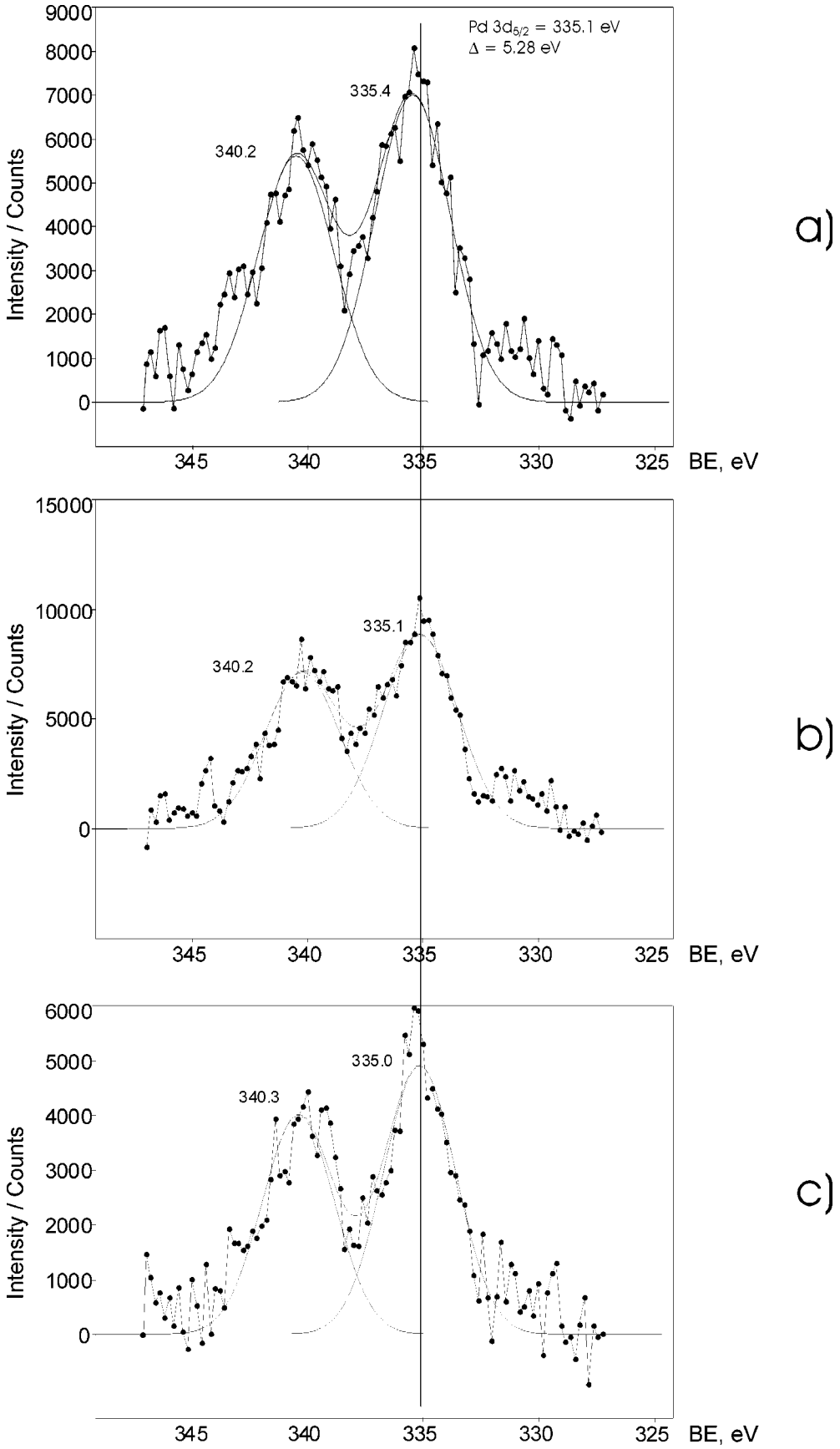

Figure 5. XPS spectra of Pd/SiO_2 prepared by CCS in "as-prepared" state (a), after teatment at 423 K in H_2 for 1 h (b), and after subsequent treatment at 573 K in H_2 for 1 h (c).

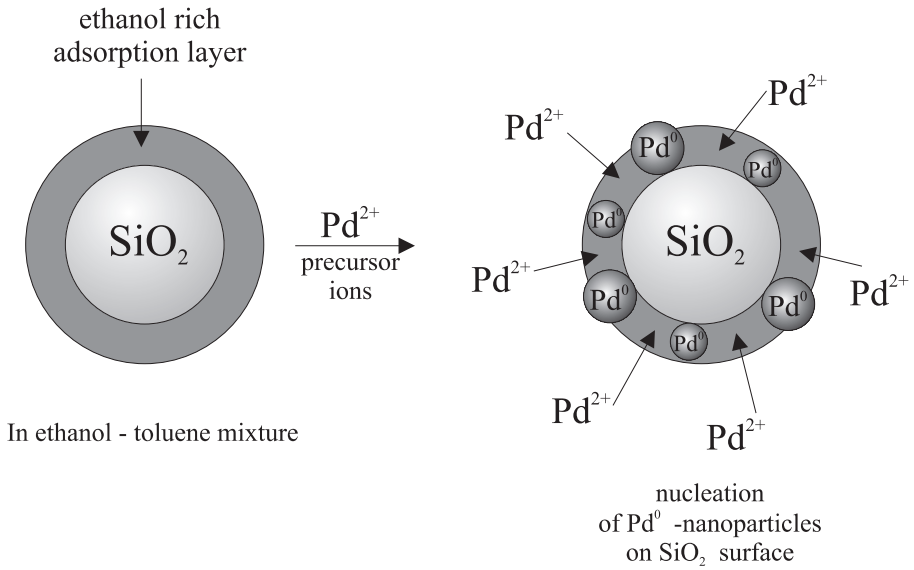

Scheme 1. Formation of Pd particles on the surface of SiO_2 particles.

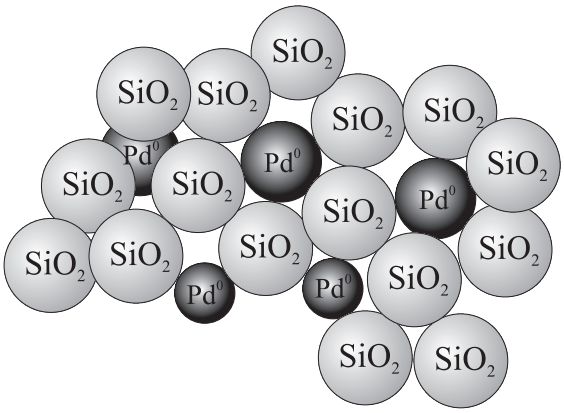

Scheme 2. Modelling the Pd and SiO_2 particles in the Pd/SiO_2 system.

is believed that during storing the samples in air the metal particles were partly oxidized.

The aim of the present work was to study, how the size of the Pd particles could be regulated by the reduction time, i.e., by the time of the particle growth. Here we must assume that the particles are growing without formation of new nuclei. Figure 6 presents the amount of palladium reduced (Pd content of the samples) versus reduction time in the given composition of the preparation mixture. Upto about 5% conversion the amount of Pd(0) increases linearly by the reduction time, around 10% conversion the reduction rate already decreases. In figure 7 the diagram shows the mean diameter of Pd particles determined by TEM and calculated from CO chemisorption data versus Pd content. The corresponding particle size data coming from TEM and CO chemisorption measurements are somewhat dissimilar. Differences in particle sizes less than 50% have no trend. It can be ascribed to the uncertainties of the measurement. In a few cases where the difference between the particles mean diameter measured by these two methods, is more than 100 or 200%, the CO chemisorption refers always to smaller Pd surface than what TEM suggests. Partial coverage of the Pd surface is assumed, and it is supported by the catalytic test, but its origin is not revealed. TONs calculated by dispersion data based on CO chemisorption are close to constant and in the same order of magnitude as measured for other supported Pd catalysts [15]. The surface of the CCS 5 sample must be heavily contaminated, because it was deactivated in several minutes in the catalytic reaction.

If one regards the mean particle diameters originated from TEM, there is a slow increase in the size of the samples with increasing Pd content. Assuming that particle growth takes place without significant nucleus formation during the reduction, and assuming that spherical particles are formed, one can calculate the increase of the Pd particle diameter (d_{Pd}) depending on the mass (m_{Pd}) of the metallic Pd(0) during the particle growth. The relationship is as follows:

$$d_{\mathrm{Pd}} = (K/N_{\mathrm{p}})^{1/3} m_{\mathrm{Pd}}^{1/3}, \tag{3}$$

where N_{p} is the number of particles, $K = 6/\pi\rho_{\mathrm{Pd}}$, ρ_{Pd} is the density of palladium.

When the number of particles is constant, the particle diameter must be in a cubic root relationship with the mass of Pd(0). The size of the samples prepared by CCS is in line with the theory (see figure 7), so we can conclude that in the preparation the particle growth is indeed the dominating factor. On the other hand, it must be stated that the particle size cannot efficiently be regulated by the reduction time. At the small Pd content region, where the slope of d_{Pd} versus m_{Pd} curve is large, investigations are limited because of the experimental difficulties. However, changing the particle number seems to be a more effective way of particle size control as can be estimated from figure 8, where the functions of $d_{\mathrm{Pd}} = f(m_{\mathrm{Pd}})$ are represented at different N_{p} values. The increasing of reduction rate by increasing of Pd ion concentration or temperature supposedly enhances the

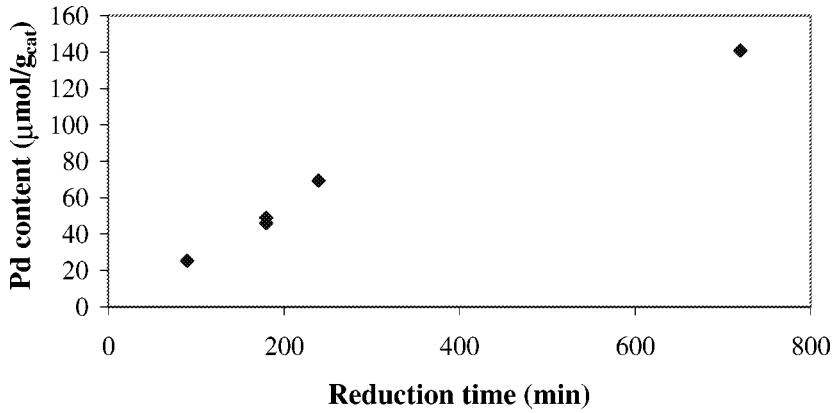

Figure 6. Relation between the amount of Pd reduced and the reduction time.

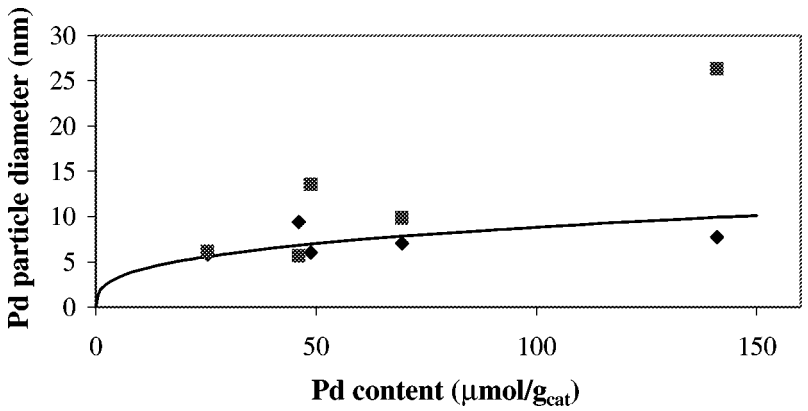

Figure 7. Relation between Pd particle size determined by TEM (♦) and calculated from CO chemisorption data (■) and Pd content in the samples CCS 1–5 and the theoretical relation (—).

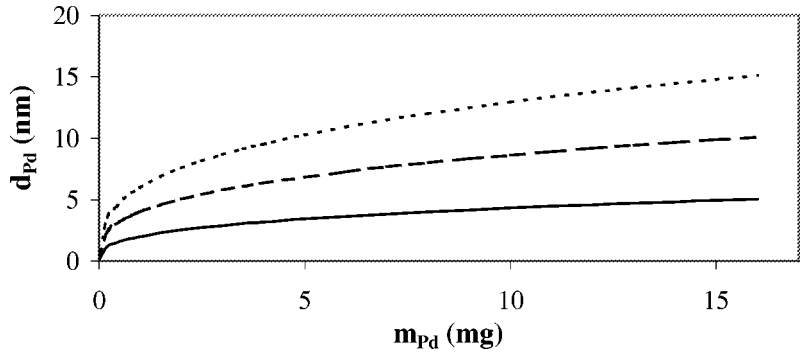

Figure 8. Theoretical change of the particle size with the increasing amount of Pd during the growth of a given number of spherical particles in the case of three different numbers of nuclei: $N_p = 200 \times 10^{14}$ (—), $N_p = 26 \times 10^{14}$ (– – –), $N_p = 8 \times 10^{14}$ (- - -).

initial nucleation rate. But the reduction rate must be under a given limit ensuring the dominancy of the particle growth during the reduction process after the initial nucleation.

If one assumes uniform particle growth all over the support surface, ideally monodisperse particle size distribution could be expected. The size distribution histograms of the Pd/SiO_2 samples prepared by CCS show, that most of the particles are in the 2–10 nm size range, which is not really narrow, but significantly narrower than in the case of the sample IMP A. Nevertheless, sample IMP B, for which the reduction temperature was smaller and the reduction time was shorter than for IMP A, has similar size distribution as CCS samples.

We have to point out that the diameters of the particles produced are bigger than the thickness of the adsorption layer where the reduction starts. Unfortunately, the thickness of the "nanoreactor"cannot limit the particle growth. This is, however, explainable if one regards that the adsorption layer cover both the support surface and the Pd particles. Ethanol must be enriched on the Pd particles

too, because the particle growth is continuing above 1 nm in diameter producing spherical particles as it is estimated from TEM images, but the composition of that layer probably differs somewhat from that on the support. This fact makes the interpretation of the preparation process even more complicated.

5. Conclusions

By controlled colloidal synthesis (CCS) monodisperse Pd particles were grown *in situ* in the adsorption layer of colloidal silica particles suspended in a toluene/ethanol binary solvent system. Comparing it with an analogous Pd/SiO_2 system prepared by a conventional method (impregnation, calcination, reduction by H_2), a sharper particle size distribution was achieved by CCS. The catalytic activity in benzene hydrogenation characterized by TON was about the same for the CCS and the "conventional" samples. The mean particle size of the samples prepared applying different reduction times varied in a relatively narrow range, which is in agreement with theoretical considerations. Changing of the number of nuclei initially produced by changing the reduction rate seems to be a more efficient way for the regulation of particle size.

Acknowledgement

The support of this research by the Hungarian Science and Research Found (grant #F-020866) is gratefully acknowledged. The authors are indebted to Mrs. Zsuzsa Koppány for the CO chemisorption measurements.

References

[1] M. Che and C.O. Bennett, Adv. Catal. 36 (1989) 55.
[2] G. Schmid, V. Maihack, F. Lautermann and S. Peschel, J. Chem. Soc. Dalton Trans. (1996) 589.
[3] B.C. Gates, L. Guczi and H. Knözinger, eds., *Metal Clusters in Catalysis*, Stud. Surf. Sci. Catal., Vol. 29 (Elsevier, Amsterdam, 1986).
[4] H. Bönnemann, Stud. Surf. Sci. Catal. 91 (1994) 185.
[5] S.T. Homeyer and W.M.H. Sachtler, J. Catal. 118 (1989) 266.
[6] M. Boutonet, J. Kizling, V. Mintsa-Eya, A. Choplin, R. Touroude, G. Maire and P. Stenius, J. Catal. 103 (1987) 95;
M. Kishida, K. Umakoshi, J.-I. Ishiyama, H. Nagat and K. Wakabayashi, Catal. Today 29 (1996) 355.
[7] A.S. Eppler, G. Rupprechter, L. Guczi and G.A. Somorjai, J. Phys. Chem. B 101 (1997) 9973.
[8] Z. Király, I. Dékány, A. Mastalir and M. Bartók, J. Catal. 161 (1996) 401.
[9] I. Dékány, L. Túri, E. Tombácz and J.H. Fendler, Langmuir 11 (1995) 2285.
[10] I. Dékány, L. Nagy, L. Túri, Z. Király, N.A. Kotov and J.H. Fendler, Langmuir 12 (1996) 3709.
[11] G. Schay, in: *Surface and Colloid Science*, Vol. 2, ed. E. Matijevic (Wiley, London, 1969) p. 155;
G. Schay, in: *Surface Area Determination*, Proc. Int. Symp., ed. D.H. Everett (Butterworth, London, 1969) p. 273.
[12] J.R. Anderson, *Structure of Metallic Catalysts* (Academic Press, London, 1975).
[13] A. Palazov, C.C. Chang and R.J. Kokes, J. Catal. 36 (1975) 338;
G. Gubotisa, A. Berton, M. Camia and N. Pernicone, Stud. Surf. Sci. Catal. 16 (1983) 431.
[14] M. Crocker, R.H.M. Herold, J.G. Buglass and P. Companje, J. Catal. 141 (1993) 713;
J.P. Collmann, L.S. Hegedus, J.R. Norton and R.G. Finke, *Principles and Applications of Organotransition Metal Chemistry* (University Science Books, Mill Valley, CA, 1987) p. 90.
[15] M.A. Vannice and W.C. Neikam, J. Catal. 23 (1971) 401;
F. Figueras, S. Fuentes and C. Leclercq, in: *Growth and Properties of Metal Clusters*, ed. J. Bourdon (Elsevier, Amsterdam, 1980) p. 525;
A. Benedetti, G. Cocco, S. Enzo, F. Pinna and L. Schiffini, J. Chim. Phys. 78 (1981) 877.